UNLIMITED

UNCLASSIFIED

ERDE 12/R/67

Copy No. 21

38

MINISTRY OF TECHNOLOGY

EXPLOSIVES RESEARCH AND DEVELOPMENT ESTABLISHMENT

REPORT No. 12/R/67

High Explosive Light Sources as Possible Laser Pumps

R.T. Bailey
J.T.A. Burton

FOR OVERSEAS RELEASE CONDITIONS SEE INSIDE COVER

WALTHAM ABBEY
ESSEX

UNCLASSIFIED

35

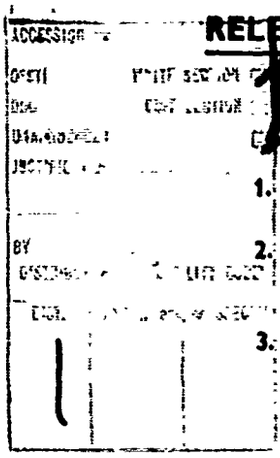

RELEASE CONDITIONS FOR OVERSEAS DISTRIBUTION

A

1. THIS INFORMATION IS RELEASED BY THE UK GOVERNMENT TO THE RECIPIENT GOVERNMENT FOR DEFENCE PURPOSES ONLY.
2. THIS INFORMATION MUST BE ACCORDED THE SAME DEGREE OF SECURITY PROTECTION AS THAT ACCORDED THERETO BY THE UK GOVERNMENT.
3. THIS INFORMATION MAY BE DISCLOSED ONLY WITHIN THE DEFENCE DEPARTMENTS OF THE RECIPIENT GOVERNMENT AND TO ITS DEFENCE CONTRACTORS WITHIN ITS OWN TERRITORY, EXCEPT AS OTHERWISE AUTHORISED BY THE MINISTRY OF TECHNOLOGY, TIL. SUCH RECIPIENTS SHALL BE REQUIRED TO ACCEPT THE INFORMATION ON THE SAME CONDITIONS AS THE RECIPIENT GOVERNMENT.
4. THIS INFORMATION MAY BE SUBJECT TO PRIVATELY-OWNED RIGHTS.

B

1. THIS INFORMATION IS RELEASED BY THE UK GOVERNMENT TO THE RECIPIENT GOVERNMENT FOR DEFENCE PURPOSES ONLY.
2. THIS INFORMATION MUST BE ACCORDED THE SAME DEGREE OF SECURITY PROTECTION AS THAT ACCORDED THERETO BY THE UK GOVERNMENT.
3. THIS INFORMATION MAY BE DISCLOSED ONLY WITHIN THE DEFENCE DEPARTMENTS OF THE RECIPIENT GOVERNMENT AND TO THOSE NOTED IN THE ATTACHED LIST, EXCEPT AS OTHERWISE AUTHORISED BY THE MINISTRY OF TECHNOLOGY, TIL. SUCH RECIPIENTS SHALL BE REQUIRED TO ACCEPT THE INFORMATION ON THE SAME CONDITIONS AS THE RECIPIENT GOVERNMENT.
4. THIS INFORMATION MAY BE SUBJECT TO PRIVATELY-OWNED RIGHTS.

C

1. THIS INFORMATION IS RELEASED BY THE UK GOVERNMENT TO THE RECIPIENT GOVERNMENT FOR DEFENCE PURPOSES ONLY.
2. THIS INFORMATION MUST BE ACCORDED THE SAME DEGREE OF SECURITY PROTECTION AS THAT ACCORDED THERETO BY THE UK GOVERNMENT.
3. THIS INFORMATION MAY BE DISCLOSED ONLY WITHIN THE DEFENCE DEPARTMENTS OF THE RECIPIENT GOVERNMENT, EXCEPT AS OTHERWISE AUTHORISED BY THE MINISTRY OF TECHNOLOGY, TIL.
4. THIS INFORMATION MAY BE SUBJECT TO PRIVATELY-OWNED RIGHTS.

D

5. THIS INFORMATION IS RELEASED FOR INFORMATION ONLY AND IS TO BE TREATED AS DISCLOSED IN CONFIDENCE. THE RECIPIENT GOVERNMENT SHALL USE ITS BEST ENDEAVOURS TO ENSURE THAT THIS INFORMATION IS NOT DEALT WITH IN ANY MANNER LIKELY TO PREJUDICE THE RIGHTS OF ANY OWNER THEREOF TO OBTAIN PATENT OR OTHER STATUTORY PROTECTION THEREFOR.
6. BEFORE ANY USE IS MADE OF THIS INFORMATION FOR THE PURPOSE OF MANUFACTURE, THE AUTHORISATION OF THE MINISTRY OF TECHNOLOGY, TIL MUST BE OBTAINED.

MINISTRY OF TECHNOLOGY

EXPLOSIVES RESEARCH AND DEVELOPMENT ESTABLISHMENT

REPORT No. 12/R/67

High Explosive Light Sources as Possible Laser Pumps

by

R.T. Bailey and J.T.A. Burton

Approved: E.G. WHITBREAD
SE

Approved for Circulation: L.J. BELLAMY
DIRECTOR

25th April 1967

WALTHAM ABBEY
ESSEX

DISTRIBUTION

EXTERNAL

TIL (30)
Dr. S.W. Bell, BDSW(R & D), through TIL

Ministry of Technology

DC/GW
DRAE (4, including Mr. P.J. Bateman, Dr. T.A. Holbeche and Mr. A.A. Wells)
DGW/X
DGW/R
DSR/L
AD/MXRD (2)
GW(G & C)3 (3) (attn. Mrs. M.G. Garrard)

Atomic Energy Authority

DAWRE

Ministry of Defence

Army Department

D/RARDE (4)
D of Arty (R & D)
Sec SAC
RMC of S, Shrivenham

Air Force Department

R.A.F.T.C., Henlow

Navy Department

DSW(N)
DGW(N)
Capt., HMS EXCELLENT
Chief Scientist, AUWE
RNC, Greenwich
NSTIC

/DISTRIBUTION (Cont'd.) .....

DISTRIBUTION (Cont'd.)

INTERNAL

D/ERDE
FS/D
Mr. G.K. Adams
SAI
SE
SH 1
SH 2
SP 1
SP 2
SCE
S/ISRG
Mr. J.T.A. Burton
Dr. J.A. Hicks
Mr. S.J. Hawkins
Dr. A.R. Osborn
File
Information Section
Archives
Library Services (2 + stock)

Further copies of this report can be obtained from the Director, Explosives Research and Development Establishment, Waltham Abbey, Essex.

CONTENTS

Reference: WAC/173/013

1. SUMMARY

The visible radiation from a thermally ionized high density plasma produced by explosively generated shock waves has been investigated as a possible laser pumping source. It is considered that the major problem is the efficiency of conversion from chemical energy to radiation in the absorption band of the laser. The study has therefore been concentrated on the mechanism of the emissive process with a view to increasing the radiation emitted in a given spectral region. The real gas thermodynamic variables behind the shock waves have been evaluated for argon and helium and used to calculate linear absorption coefficients based on Unsöld-Kramers' theory. Using Kirchhoff's law, the radiant intensities at the surfaces of optically thick argon and helium plasmas at 20,000°K have been calculated and compared with observed values in the visible spectral region. The effects of various parameters such as gas composition, pressure and shock velocity on the spectral radiance have been studied experimentally. It is concluded that the radiation from explosively shocked noble gases is essentially black body in nature.

2. INTRODUCTION

In recent years there has been considerable interest in the use of lasers for producing transient high radiation densities. At present, high energy laser systems are relatively inefficient and very large input energies are needed if high output energies are required. Also, since the available pumping times for present day laser materials are short, this energy must be supplied at a very high rate.

High explosives are probably the most compact, cheapest and lightest energy sources available; the explosive 60/40 RDX/TNT contains about 0.77×10^6 joules kg^{-1}. To store the equivalent energy, a capacitor bank would have to be at least 50,000 times as large in both volume and weight. However, since explosives are destructive in nature they are useful only in certain classes of application.

The use of explosive energy to pump lasers poses the problem of converting the chemical energy of the explosive into radiation of the appropriate frequency. Of the several methods available only one is considered here; an explosively generated shock wave in a monatomic gas is intensely luminous and the light may be used directly to pump lasers. This report describes a study of the mechanism by which the energy of the expanding detonation products is converted into radiation.

/As .....

As a starting point in this investigation, the argon flash bomb was evaluated. This is a simple device designed to meet the needs of high speed photography and consists of a cardboard box containing a thin slab of explosive at one end and fitted with a cellophane window at the other end. When the air is flushed out with argon and the explosive is detonated several hundred million candlepower is produced for about 10^{-4} sec. Assuming for the moment that the radiative intensity corresponds to that of a black body at 20,000°K the total energy radiated is about 9×10^5 watts cm^{-2} for 10^{-4} sec. or 90 joules cm^{-2} of radiating surface. Considering a flash bomb containing a slab of RDX/TNT 1 cm thick the chemical energy liberated is about 6.4×10^3 joules cm^{-2} of explosive. This leads to an overall conversion efficiency of 1.4 per cent from stored chemical energy to total radiated energy.

3. THEORETICAL CONSIDERATIONS

In this Section, the theoretical aspects of the energy conversion process are studied with a view to predicting the optimum conditions necessary for obtaining maximum radiance, in a given frequency interval, for a given explosive/gas system. The emphasis is placed more on obtaining maximum spectral intensity than on conversion efficiency from chemical to radiant energy.

3.1 Equilibrium Shock Wave Calculations

An essential prerequisite to the understanding of the radiative properties of a shock-heated gas is a knowledge of the equilibrium real gas thermodynamic variables behind the shock front. Under the extreme conditions produced by high explosives, deviations from perfect gas behaviour may result from thermal excitation and ionization of the gas behind the shock front. These difficulties can be overcome by the introduction of quantum statistical mechanics of the microcanonical assembly into the shock wave calculations to allow for these real gas effects.

There have been many such calculations for plasmas produced by shock waves, particularly for low pressures (1), but little attention has been given to conditions of very high pressure and temperature behind the shock front. Bond (2) has calculated the equilibrium properties of argon for ambient pressures of 10 torr and 593 torr for incident shock velocities of between 3×10^5 cm sec^{-1} and 9×10^5 cm sec^{-1}. Lowering of the first ionization potential was not taken into account in his calculations and at the higher pressures and velocities considered by him this could lead to considerable error. Second ionization and excitation were also neglected. Since accurate values of temperature, degree of ionization and particularly electron density are essential if meaningful absorption coefficients are to be evaluated, the physical bases of existing equilibrium shock wave calculations were reviewed.

/Considerable .....

Considerable progress has been achieved in this field recently, particularly with regard to the development of a consistent physical model (1,3). The results of preliminary calculations for argon and helium are reported here. It should be emphasised that these calculations assume that equilibrium conditions maintain behind the shock front. The problem of energy relaxation is not considered, the assumption being made that the equilibrium state is not influenced by the physical processes that govern the approach to equilibrium.

For a monatomic gas, the equilibrium conditions are determined by the equations for the conservation of mass-flow, momentum and total energy across the shock together with the equation of state, the Saha equation, and the equation for the ionization potential.

Using the flow regimes shown in Fig. 1, based on a stationary shock, and assuming no ionization in the undisturbed gas ahead of the shock front, the conservation equations can be written in the form*:

$$\rho_1 u_1 = \rho_0 u_0 \qquad \text{..... 1}$$

$$P_1 + \rho_1 u_1^2 = P_0 + \rho_0 u_0^2 \qquad \text{..... 2}$$

$$RT_1\left[\frac{5}{2}(1+\alpha_1) + (1-\alpha_1)\,T_1\frac{\partial}{\partial T}(\ln Q_0^{el}) + \alpha_1 T_1 \frac{\partial}{\partial T}(\ln Q_1^{el})\right] + \alpha_1 \frac{\chi}{k_A} + \frac{u_1^2}{2} = \frac{5}{2}RT_0 + \frac{u_0^2}{2} \qquad \text{..... 3}$$

where the subscript o refers to conditions in the undisturbed gas and the subscript 1 to the equilibrium conditions behind the shock front.

The equations of state are

$$P_0 = \rho_0 R T_0 \qquad \text{..... 4}$$

and

$$P_1 = (1+\alpha_1)\,\rho_1 R T_1 \qquad \text{..... 5}$$

where R is the gas constant per unit mass. The Saha equation can be written

/in .....

*To achieve some economy in presentation the symbols in common use are not defined in the text but all definitions are tabulated in the Appendix.

in the form:

$$\frac{\alpha_1^2}{1-\alpha_1^2} P_1 = \frac{(2\pi M_e)^{\frac{3}{2}}}{h^3} K^{\frac{5}{2}} \cdot 2 \cdot \frac{Q_1}{Q_o} T^{\frac{5}{2}} \exp\left(\frac{-\chi}{KT}\right) \quad \ldots\ldots 6$$

The ionization potential χ is equal to the ionization potential χ_o for the isolated atom, reduced by $\Delta\chi$ due to the surrounding plasma. The equation for the lowering of the ionization potential used in the preliminary calculations was that favoured by Pomerantz (4), who critically reviewed the literature on this topic. This equation, which was derived by Ecker and Weizel (5), is given in the form:

$$\Delta\chi = 0.67 \times 10^{-6} N_e^{\frac{1}{3}} + 0.37 \times 10^{-7} \left(\frac{N_e}{T}\right)^{\frac{1}{2}} \quad \ldots\ldots 7$$

The first term on the r.h.s. which is generally the dominant term represents the ionization potential lowering due to the plasma microfield (the Unsöld term), whilst the second term accounts for the energy level lowering effects arising from plasma polarization. This theory has recently been criticized on the grounds that it leads to too large a value of $\Delta\chi$ for the densities involved in most laboratory plasmas (6,7).

The electron density is given by:

$$N_e = \frac{\alpha_1}{1-\alpha_1} \frac{P_1}{kT} \quad \ldots\ldots 8$$

The calculation of electronic partition functions is an astrophysical problem of long standing. The partition function is defined by the relationship

$$Q^{el} = \sum_{n=0} g_n \exp\left(\frac{-\epsilon_n}{kT}\right) \quad \ldots\ldots 9$$

where g_n is the statistical weight or degeneracy of an atomic energy level whose energy is ϵ_n. The summation is formally over all available energy levels. There are two main problems involved in the calculation of the partition function. The first is the fundamental problem of its divergence. This arises because there exists for a given atom an infinite number of discrete electronic states converging to a continuum, and since the excitation energies of these states are finite the partition function diverges. This problem is generally overcome by employing some kind of cut-off procedure whereby the summation of the energy levels is terminated at a specified value of excitation energy. In some cases,

/the .....

the partition functions are terminated at a value determined by the equation for the lowering of the ionization potential. The second problem, which arises from the lack of available information on the electronic energy levels of the atoms and ions, is usually ignored and only the available tabulated energy levels are included in the summation (8). Recently, however, McChesney (9) has estimated the missing energy levels and evaluated their effect on the calculated equilibrium thermodynamic properties of shock-heated xenon.

3.2 Shock Wave Calculations for Argon and Helium

The equilibrium properties of explosively shocked argon and helium, initially at atmospheric pressure, have been calculated. In these calculations, no attempt was made to compute exact partition functions. In the case of argon, the generally used approximation $Q_o^{el} = 1$ and $Q_1^{el} = 6$ was used, while with helium, due to the very high excitation energies of the first excited states (19.8 eV), the partition functions were approximated to the statistical weights of the ground states of the atoms and first ions.

In these calculations, the following assumptions were made:

(i) the flow phenomena are adequately described by hydrodynamic theory for a one-dimensional shock wave with heat conduction, radiative cooling, and viscosity neglected;

(ii) thermal equilibrium exists in finite regions behind the shock front;

(iii) the hot gas behind the shock front consists of a perfect gas mixture of atoms, electrons, and first ions; and

(iv) reflection of the shock wave occurs at a perfectly rigid wall.

In the preliminary calculations, multiple ionization and electronic excitation of the atoms and ions were ignored. This should not lead to appreciable error in the case of helium. However, due to the lower excitation and ionization energies of the argon atom, there will be appreciable second ionization and electronic excitation which could lead to error, particularly in the calculated temperature and electron density.

Since the conditions in the undisturbed gas ahead of the shock are known, and the shock velocity u_o is easily measured, Equations 1 to 6 can be solved by an iterative procedure. Initial estimates for the pressure and degree of ionization behind the shock wave were based on the assumptions that half the energy behind the shock front goes into ionization in the case of argon and that the majority of the energy in front of the stationary shock is kinetic energy. This leads to the approximate forms of Equations 2 and 3, viz.

/Equation .....

$$P_1 = \rho_o u_o^2 \qquad \ldots\ldots 10$$

and

$$\alpha_1 \frac{\chi}{M_A} = \frac{u_o^2}{4} \qquad \ldots\ldots 11$$

With these initial estimates Equations 1 to 6 were solved with $\chi = \chi_o$. From the approximate values of α_1, P_1 and T_1 thus calculated, Equations 7 and 8 are used to determine the first approximation of χ. Equations 1 to 6 are then resolved with the new value of χ. This process is repeated until the variables converge to the desired degree of accuracy.

The shock equations were solved for a shock wave propagating at 8.3×10^5 cm sec^{-1} (Mach 27) into atmospheric pressure argon. After about twenty iterations, the following values were obtained, $T_1 = 19{,}880°K$, $\alpha_1 = 0.75$, $\rho_1 = 1.39 \times 10^{-2}$ g cm^{-3}, $P_1 = 1.009 \times 10^9$ dyn cm^{-2} and $N_e = 1.57 \times 10^{20}$ cm^{-3}.

Equations 1 to 6 were also solved for atmospheric pressure helium with an incident shock velocity of 10.1×10^5 cm sec^{-1}. Since the Mach number (about 10) and degree of ionization are low, no lowering of the ionization potential was considered. In fact, the calculated thermodynamic variables differed only slightly from those obtained using the usual Rankine-Hugoniot equations for an ideal gas. The calculated values were $T_1 = 9465°K$, $\alpha_1 = 2.7 \times 10^{-6}$, $\rho_1 = 1.66 \times 10^{-4}$ g cm^{-3}, $P_1 = 1.27 \times 10^8$ dyn cm^{-2} and $N_e = 2.65 \times 10^{16}$ cm^{-3}.

In the case of reflected shocks, an additional equation is needed to describe the boundary conditions imposed by the reflecting surface, i.e. the gas particles behind the reflected shock are rendered stationary. In a coordinate system moving with the reflected shock, this equation can be written

$$u_{oR} - u_{1R} = u_o - u_1 \qquad \ldots\ldots 12$$

where u_{oR} and u_{1R} are the flow velocities of the gas entering and leaving the reflected shock.

With the aid of Equations 1 to 6 and the boundary condition described by Equation 12, the physical variables behind the reflected shock in helium were obtained. They were $T = 20{,}370°K$, $\alpha = 9.6 \times 10^{-3}$, $\rho = 6.45 \times 10^{-4}$ g cm^{-3}, $P = 1.009 \times 10^9$ dyn cm^{-2} and $N_e = 2.43 \times 10^{18}$ cm^{-3}. No consideration has yet been given to the problem of the lowering of the ionization potential. The inclusion of ionization potential lowering effects would result in a somewhat higher degree of ionization and electron density and a lower temperature.

/Equilibrium .....

Equilibrium shock wave calculations are in progress which allow for multiple ionization and excitation and the lowering of the ionization potential. These effects are likely to be of considerable importance in, for example, the reflected shock in argon. The Debye-Huckel theory of point charges as applied by Griem (7) for multiple ionized plasmas, is being used as the basis of these calculations. This theory provides an internally consistent physical model for lowering of the ionization potential and terminating the partition function.

3.3 Radiant Emission from the Hot Dense Plasma

The energy radiated from a hot dense plasma arises from three types of spectral transition. These are

(a) bound-bound transitions which give rise to the ordinary line spectra emitted by atoms and ions,

(b) free-bound transitions consisting of the recombination of "free" plasma electrons into bound states of the positive ions with the emission of continuous radiation, and

(c) free-free transitions which also give rise to continuous radiation. This process can be described classically by the deceleration of electrons in hyperbolic orbits in the fields of positive ions, thereby transforming kinetic energy of the electron into radiation. This is the well known Bremsstrahlung radiation.

In view of the extreme conditions of temperature and pressure in the plasma, line spectra will be broadened and shifted by perturbation of the energy levels by particles in the neighbourhood of the radiating atom. Also, when there is an appreciable degree of ionization, the electrical fields of nearby ions will give rise to Stark broadening. Trapped magnetic fields in the plasma may also lead to Zeeman splitting. Under conditions of very high pressure and temperature, therefore, most of the line radiation will be smeared out to such an extent that it is masked by the continuum. Also, when the degree of ionization is high, the occupation number for a particular excited state is low and hence the line it emits is weak and merges more easily with the continuous background. Finally, the rare gases contain a large number of closely spaced lines which may be expected to overlap under these conditions. In this type of plasma, therefore, the contribution of bound-bound transitions to the total emitted intensity will be small and is neglected in the intensity calculations.

In the case of optically thick plasmas, in local thermodynamic equilibrium, emitted spectral intensities are best obtained from the continuous absorption coefficient using Kirchhoff's law and correcting for stimulated emission. Allowance must also be made for absorption of radiation by the plasma.

/Lambert's .....

Lambert's law for the absorption of radiant energy is

$$I = I_o \exp(-K\ell) = I_o \exp(-N\sigma\ell) \quad \text{..... 13}$$

where I_o is the intensity of the incident beam; I is the intensity of the beam after it traverses a distance ℓ of the gas; K is the linear absorption coefficient of the gas; σ is the cross-section for this absorption; and N is the density of the absorbing particles. N and σ must be individually considered for each of the types of radiation absorption processes and if there are several for the frequency or frequency region of interest, they must be summed.

Assuming that the concept of local thermodynamic equilibrium is valid, or equivalently that Kirchhoff's law holds, the gaseous emissitivity of the plasma can be written as (10)

$$\epsilon = 1 - \exp(-K\ell) \quad \text{..... 14}$$

Following Breene and Nardone (11) a factor β is introduced into the exponent giving

$$\epsilon = 1 - \exp(-\beta K\ell) \quad \text{..... 15}$$

In deriving the above emissivity expressions, one must consider the radiation arriving at the surface of an emitting gaseous layer after its augmentation and diminution during passage through the layer along a particular path. At a given point on the boundary, however, radiation is arriving along any number of paths and an integration over these paths is necessary. For paths of the order of a few centimetres and smaller, it has been found that a value of $\beta = 1.8$ approximates the results of angular integration.

The spectral radiance is then obtained by multiplication with the Planck function

$$I_\nu = \epsilon_\nu B_\nu d\nu = B_\nu[1 - \exp(-\beta K\ell)]d\nu \quad \text{..... 16}$$

where $$B_\nu d\nu = \frac{2h\nu^3}{C^2}[\exp(h\nu/kT) - 1]^{-1}d\nu$$

/3.4 .....

3.4 Unsöld-Kramers Theory

The problem is now resolved into one of calculating the continuous absorption coefficient K_ν. In principle, K_ν can be calculated from quantum mechanical considerations, but to the present time this has only been accomplished for one-electron systems. Unsöld (12) using the classical Kramers (13) theory, has developed a theoretical expression for Bremsstrahlung and recombination radiation. According to this theory, the free-free absorption index of radiation of frequency ν in the field of a singly charged ion is given by

$$K_\nu = \frac{16\,\pi^2 e^6}{3\sqrt{3}\,ch(2\pi m_e)^{\frac{3}{2}}} \cdot \frac{N_e^2}{(kT)^{\frac{1}{2}}} \cdot \frac{1}{\nu^3} \int_0^\infty \exp(-a)da \qquad \text{..... 17}$$

$$= 3.70 \times 10^8 \frac{N_e^2}{T^{\frac{1}{2}}} \cdot \frac{1}{\nu^3} \qquad \text{..... 18}$$

where N_e is the electron density; $a = m_e V^2/kT$, V is the electron velocity and T is the electron temperature.

If local thermodynamic equilibrium pertains, then Equation 18 can be generalized to include free-bound absorption. For this purpose, the lower integration limit should not be zero but $-a = -h\nu/kT$, corresponding to the limit of photoelectric absorption of frequency ν. The total absorption index, taking account of both free-free and free-bound absorption of a single charged ion, will have the form,

$$K_\nu = \frac{16\,\pi^2 e^6}{3\sqrt{3}\,ch(2\pi m_e)^{\frac{3}{2}}} \cdot \bar{g} \cdot \frac{N_e^2}{(kT)^{\frac{1}{2}}} \cdot \frac{1}{\nu^3} \int_{-a}^\infty \exp(-a)da \qquad \text{..... 19}$$

$$= 3.70 \times 10^8\, \bar{g} \cdot \frac{N_e^2}{T^{\frac{1}{2}}} \cdot \frac{1}{\nu^3} \exp(h\nu/kT) \qquad \text{..... 20}$$

In the case of an optically thick plasma, induced emission must be considered. The absorption coefficient corrected for induced emission, can be expressed by

$$K = 3.70 \times 10^8\, \bar{g} \cdot \frac{N_e^2}{T^{\frac{1}{2}}} \cdot \frac{1}{\nu^3} [\exp(h\nu/kT) - 1] \qquad \text{..... 21}$$

/The .....

The factor $\bar{g}$ has been introduced to correct for the dissimilarity between the atom and hydrogen, that is, partial penetration of electrons into the shell of the atom.

The applicability of this equation to specific atoms can be evaluated by considering the model term scheme shown in Figure 2. In his treatment, Unsöld assumed recombination into hydrogen-like states which were sufficiently dense to permit the sum over discrete states to be replaced by an integral. Thus Equation 22 gives the absorption index up to a limiting frequency ν_g, corresponding to an energy $h\nu_g$. The sequence of terms is considered as being sufficiently dense up to the term $h\nu_g$ (measuring from the ionization limit), to replace term summation by integration, the contribution of terms below $h\nu_g$ must be accounted for by individual summation. If no terms exist between $h\nu_g$ and the ground state, the lower boundary of the integral in Equation 19 (for $\nu > \nu_g$) will remain constant and equal to $-a = -h\nu_g/kT$. In this case, the absorption coefficient will be given by

$$K_\nu = 3.70 \times 10^8 \bar{g} \cdot \frac{N_e^2}{T^{\frac{1}{2}}} \cdot \frac{1}{\nu^3} [\exp(h\nu_g/kT) - 1] \qquad \ldots\ldots 22$$

and the absorption index will decrease according to $\frac{1}{\nu^3}$. A comparison of Equations 18 and 21 gives the ratio of total to free-free absorption coefficient as

$$\bar{g} [\exp(h\nu/kT) - 1]$$

Assuming, in the general case, that $\bar{g} = 1$, at a temperature of 20,000°K, free-free absorption contributes 10 per cent of the total at 3000 Å and 43 per cent at 6000 Å. At 9000 Å, the contribution of Bremsstrahlung absorption reaches 80 per cent of the total. The contribution of free-free absorption is thus small in the ultra-violet region but increases with wavelength. It also increases in importance at higher temperatures. Bremsstrahlung continuum will therefore play an important role under the conditions of interest to us.

An examination of the energy level diagram for the unperturbed argon atom, reveals the existence of a continuous sequence of terms between the ionization limit and the $3d^6$ term at $\nu_1^* = 16,873$ cm^{-1}. There is then a window of the order of 3000 cm^{-1} in the term sequence until the next series of terms. This group of levels starts at $\nu_2^* = 19,818$ cm^{-1} and ends at $\nu_3^* = 24,439$ cm^{-1}. A second window of about 9000 cm^{-1} exists between the $2p^{10}$ level at $\nu_3^* = 24,439$ cm^{-1} and the last sequence of terms starting at $\nu_4^* = 33,141$ cm^{-1} and ending at $\nu_5^* = 35,397$ cm^{-1}. There are no terms between ν_5^* and the ground level.

/The .....

The absorption coefficient should therefore be determined by Equation 21 up to a limiting frequency (5×10^{14} sec^{-1}), corresponding to the interval between the ionization limit and the $3d^6$ term. For frequencies between ν_1^* and ν_2^*, the absorption index will vary according to Equation 22. To account for the dense sequence of terms beginning at ν_2^* and ending at ν_3^*, the absorption index will have the form (leaving out the induced emission term for clarity)

$$K_\nu = 3.7 \times 10^8 \frac{\bar{g}}{\nu^3} \cdot \frac{N_e^2}{T^{\frac{1}{2}}} \left[e^{\frac{h\nu_1^*}{kT}} - e^{\frac{h\nu_2^*}{kT}} + e^{\frac{h\nu^*}{kT}} \right] \quad \ldots\ldots 23$$

for $\nu^* > 24{,}439$ cm^{-1} to $\nu^* = 33{,}141$ cm^{-1} the absorption coefficient will be determined by the expression

$$K_\nu = 3.70 \times 10^8 \frac{\bar{g}}{\nu^3} \cdot \frac{N_e^2}{T^{\frac{1}{2}}} \left[e^{\frac{h\nu_1^*}{kT}} - e^{\frac{h\nu_2^*}{kT}} + e^{\frac{h\nu_3^*}{kT}} \right] \quad \ldots\ldots 24$$

for the frequency region from ν_4^* to ν_5^* the index will have the form

$$K_\nu = 3.70 \times 10^8 \frac{\bar{g}}{\nu^3} \cdot \frac{N_e^2}{T^{\frac{1}{2}}} \left[e^{\frac{h\nu_1^*}{kT}} - e^{\frac{h\nu_2^*}{kT}} + e^{\frac{h\nu_3^*}{kT}} - e^{\frac{h\nu_4^*}{kT}} + e^{\frac{h\nu^*}{kT}} \right] \quad \ldots\ldots 25$$

and for frequencies $\nu^* > 35{,}397$ cm^{-1} the appropriate expression will be

$$K_\nu = 3.70 \times 10^8 \frac{\bar{g}}{\nu^3} \cdot \frac{N_e^2}{T^{\frac{1}{2}}} \left[e^{\frac{h\nu_1^*}{kT}} - e^{\frac{h\nu_2^*}{kT}} + e^{\frac{h\nu_3^*}{kT}} - e^{\frac{h\nu_4^*}{kT}} + e^{\frac{h\nu_5^*}{kT}} \right] \quad \ldots\ldots 26$$

3.5 Theoretical Absorption Coefficient for Argon

The calculated absorption index for argon using T = 19,880°K, $N_e = 1.57 \times 10^{20}$ cm^{-1} and $\bar{g} = 0.9$, is shown in Figure 3. It is compared with the absorption coefficient, calculated assuming Equation 22 is valid, down to a wavelength of 2000 Å. This assumption was made by Petschek et al. (14), who noted that the capture of electrons with energies greater than about 3/2 kT to the first excited state, will be fairly infrequent. The capture of electrons to the ground state can be neglected. The first excited state of argon is

/about .....

about 4.2 eV below the ionization limit and at a temperature of 20,000°K, 3/2 kT corresponds to about 2.6 eV. This leads to an upper frequency cut-off which corresponds to the frequency interval $\Delta\bar{\nu}$ given by

$$h\Delta\nu = 6.8 \text{ eV}$$

Thus Equation 22 should be valid for a frequency interval of about 6.8 eV.

In high density ionized plasmas, however, the lowering of the ionization limit will shift the cut-off frequency to a lower value. Since accurate values of the reduced ionization potential are not available at present, this was not taken into consideration. This could lead to appreciable error when large reductions in the ionization potential exist.

3.6 Theoretical Absorption Coefficient for Helium

Using Equation 22, the absorption coefficient for helium at a wavelength of 5000 Å was calculated for incident and reflected shocks. Behind the incident shock wave (for T = 9465°K and $N_e = 2.65 \times 10^{14}$ cm^{-3}) $K_\nu = 2.6 \times 10^{-8}$ cm^{-1}, and behind the reflected shock (for T = 20,370°K and $N_e = 2.43 \times 10^{18}$ cm^{-3}), $K_\nu = 0.29$ cm^{-1}. These represent minimum values of absorption coefficient since the lowering of the ionization potential was not taken into account in calculating the temperature and electron density. The effect of the fine structure of the helium spectrum on the absorption coefficient is not evaluated here.

3.7 Calculated Radiant Emission

(a) Argon

The variation of emissivity (calculated from Equation 15) with depth of emitting layer at a wavelength of 5000 Å, is illustrated in Figure 4. The optical depth (the thickness of plasma which is contributing directly to the observed spectral intensity) is about 0.06 mm. When Equation 16 is valid, it is apparent that, if the thickness of the emitting layer is greater than the optical depth at a given wavelength, then the plasma should radiate as a black body at the equilibrium temperature. It also follows that, if energy relaxation times are negligible behind the shock front, the rise time of the radiation at 5000 Å should be about 10^{-8} sec and the continuum intensity profile should resemble that of the emissivity curve shown in Figure 4. The ionization relaxation times behind the shock front were calculated from the expression

$$P_{T_1} = 0.156 \exp(87{,}000/T)$$

/where .....

where P is the pressure in torr and τ_i is the ionization relaxation time in microseconds. Using this equation, τ_i was found to be 1.6×10^{-8} sec. This expression was obtained by Petschek and Byron (15) using high purity argon and their results indicate a marked decrease in relaxation times when less pure gas was employed. The calculated relaxation time, therefore, represents a maximum value and the actual time is probably considerably less. Electrons ejected into the argon from the detonating explosive will also reduce the relaxation time. Energy relaxation times are therefore probably negligible compared with the radiation rise times.

(b) Helium

Since the helium behind the incident shock wave has a very low absorption coefficient, its emissivity will be low and very little radiation will be observed for emitting layers of a few centimetres and less. The variation of emissivity with thickness of helium plasma at 5000 Å behind the reflected shock wave, is shown in Figure 5. The optical depth is about 10 cm, but this must be regarded as a maximum value.

4. SPECTRAL MEASUREMENTS

4.1 Spectroscopic Techniques

The absolute intensity and spectral distribution of the energy radiated by shock-heated gases were measured using a Hilger medium quartz spectrograph equipped with photoelectric recording facilities. The intensity of the radiation from the shock-heated plasma was compared at six selected narrow wavebands in the visible spectral region with that of a tungsten ribbon-filament lamp, previously calibrated by the National Physical Laboratory for brightness temperature against current. Identical optics were used for each of the two radiators in each experiment, so that, in calibrating the photomultipliers, the spectrograph and the associated optics were also calibrated. Reflective optics were used to focus the radiation on to the entrance slit of the spectrograph. The spectral intensity of the lamp at the desired wavelength and temperature was calculated employing data on the emissivity of tungsten given by De Vos (16). The output of each photomultiplier was displayed as a function of time on an oscilloscope and recorded photographically, the overall rise-time of the equipment being 15 nanosec. To achieve a wide range of light sensitivities, the photomultiplier anode loads were varied. Since the photomultipliers were calibrated at a continuous low output current level and then used to measure high current pulses, care was taken to operate the tubes only on the linear portions of their response curves. There are several possible sources of error in the measurements, such as error in ribbon lamp brightness temperature (± 7 degC), short-term drift of the photomultiplier sensitivities, uncertainties in the standard lamp current measurement and in the positioning of the lamp, so that a precise determination of error is difficult. However, the maximum error in intensity measurement is probably less than 15 per cent.

/4.2 .....

4.2 Continuum Intensity Measurements

The radiative properties of argon heated by shock waves generated by various detonating high explosives were investigated. The hot plasma was viewed normal to the direction of the shock front. Radiation reaching the spectrometer originated from only a small area about 2 mm x 0.2 mm at the centre of the shock front. Interference from edge effects arising from interaction of the shock wave with the walls of the container were thus minimised. The effects of the high explosives used to drive the shock on the continuum intensity was examined in the apparatus shown in Figure 6. The results obtained using argon at 1 atm pressure are shown in Figure 8. In the visible spectrum the radiation is similar to that from a black body at about 21,000°K. Little significant difference in intensity or spectral distribution was found using HMX, RT (a cast explosive containing about 60 per cent RDX and 40 per cent TNT), tetryl or a tetryl/TNT mixture although HMX gave on the average more light than RT. Several experiments were generally performed for each explosive composition. There was a variation of up to 20 per cent in the intensity using the same explosive. Part of this is due to experimental error but variations in the explosive charge such as composition, uniformity and physical condition probably also contribute.

The radiation from different shocked noble gases was compared using the experimental arrangement illustrated in Figure 7. Spectroscopic grade gases were sealed into the glass tubes at a pressure of 440 torr, using high vacuum techniques, and then shocked by charges of RT. The impurity level was less than 10 ppm for A, Ne and He while Kr and Xe were 99.5 per cent pure, the balance being Xe and Kr respectively. In the case of argon, krypton and xenon, intense radiation was emitted from behind the incident shock waves, with about a 50 per cent increase in intensity on reflection at the end window. However, the rise times of the radiation varied considerably, decreasing in the order argon (7.5 μsec), krypton (1 μsec) and xenon (0.1 μsec). The duration of the reflected shock also decreased in the order of increasing molecular weight from helium (2 μsec) to xenon (0.1 μsec). Typical records are illustrated in Figures 9 and 10. No light emission was observed from behind the incident shock waves in neon and helium, but on reflection at the end window of the tube a pulse of radiation comparable in intensity to that obtained from argon was observed. The observed radiancies, which are compared in Figure 11, differed by less than a factor of two (two experiments were performed for each gas).

Experiments were performed with shock waves generated by the explosion of RT in cylinder quality helium, using an apparatus similar to that shown in Figure 6. The pathlength of helium was 23 cm. Very little radiation was emitted from behind the incident shock, but on reflection a sharp pulse of radiation lasting for about 2.5 μsec was obtained. A typical record at two of the wavelengths is shown in Figure 12. It is apparent from the record that the radiation is cut off by the contact surface before the maximum intensity is attained.

/4.3 .....

4.3 Streak Photographs and Shock Velocities

A Beckman and Whitley Model 339 streak camera was used to measure the velocity of the incident shock waves and of the contact surface between the explosive and the gas. The depth of the emitting layer behind the incident and reflected shocks was also measured. The streak photograph of RT detonating into atmospheric pressure argon, Figure 13A, shows the distances of the shock front and contact surfaces as a function of time. The streak camera slit was oriented parallel to the tube axis. Figure 14 sets out the interpretation of the streak photographs obtained. The incident shock wave propagates down the column of argon at almost constant velocity until it meets the end window of the tube when it is reflected back into the hot gas. No increase in intensity is detectable when the incident shock is reflected. The thickness of the emitting gas layer is determined by the velocity of the contact surface which rapidly cools the hot gas, quenching the radiation. The maximum thickness of hot plasma at the end of the tube was found to be 1.5 cm, whilst the calculated value for this length of tube was 1.2 cm (using the particle velocity computed in Section 3). If this difference is significant, it may mean that the hot gas is not quenched immediately by the explosive products. The thickness of the reflected shock-heated gas will of course depend on the relative velocities of the reflected shock wave and the contact surface.

With helium (Figure 13B) no radiation was observed from the incident shock front but the gas behind the reflected shock was highly luminous. A fairly sharp quenching was observed when the contact surface reached the radiating plasma but the gas continued to radiate at a much lower level for some time. No satisfactory explanation of this phenomenon has yet been formulated.

5. DISCUSSION

It was shown in Section 3.3 that if the mean free path for radiation of a given frequency was less than the depth of the emitting region the emitted intensity will be that of a black body. From the very rapid rise times of the radiation in argon shocked by RT (<0.1 μsec) the optical depth must be smaller than 0.5 mm and is probably considerably less. Furthermore, since the plasma achieves a depth of about 15 mm after traversing 15 cm of gas it should radiate according to the black body law. The observed spectral distribution (Figure 8) closely approximates to that of a black body at 21,000°K.

In view of the high electron concentration in the argon plasma, absorption of radiation will be very high. This results in a much greater cooling time for the plasma than if it were optically thin. Assuming black body radiation, the natural radiative cooling time of the argon plasma is estimated to be greater than 500 μsec. Since the plasma is only allowed to radiate for a short time before it is quenched by the contact surface, which follows the shock front very closely, this represents a major energy loss process and source of inefficiency.

/To .....

To obtain a high radiance a high temperature is necessary, but increasing the shock velocity in argon will not have much effect on radiance since this will mainly result in increased ionization and a smaller optical depth. In effect, the argon temperature is buffered by thermal ionization. However, if the shock velocity is sufficient to ionize most of the argon atoms, then an abrupt rise in temperature should occur before second ionization becomes appreciable. It would appear preferable at first sight, to employ a gas of high ionization potential such as helium but unfortunately very high shock velocities are necessary with helium in order to produce a Mach number comparable to that in argon. Neon might prove to be a suitable compromise gas. An alternative approach would be to choose a material of very low first ionization potential such as caesium which is completely ionized at comparatively low temperatures. Since the second ionization potential is high (23.4 eV) it should be possible to produce a high temperature, optically dense plasma with moderate shock velocities. Unfortunately, there are severe practical problems associated with the use of caesium vapour.

High temperature black body sources emit most of their radiant energy in the extreme ultra-violet region but this is of no use for pumping the majority of laser materials. The conversion of this energy into visible radiation would result in a major improvement in the efficiency of the source. Experiments with fluorescent convertors have so far proved inconclusive. A more promising approach would be to utilize the absorbing characteristics of the gas ahead of the shock wave to tailor the spectral distribution to that of the pumping band of a given laser, perhaps by the addition of small amounts of additives. In this way it might be possible to achieve a non-equilibrium spectral distribution.

6. ACKNOWLEDGEMENTS

The authors gratefully acknowledge helpful discussions with Mr E.G. Whitbread, Dr. J.A. Hicks and Mr. S.J. Hawkins.

/6. .....

7. BIBLIOGRAPHY

1. M. McChesney, Canad J. Phys., 1964, 42, 2473.

2. J. Bond, Los Alamos Rept. 2A - 1603, 1954; Phys. Rev., 1957, 105, 1683.

3. E.A. McLean, C.E. Faneuff, A.C. Kolb and H.R. Griem, 1960, Phys. Fluids, 3, 843.

4. J. Pomerantz, J. Quant. Spectr. Rad. Transfer, 1961, 1, 185.

5. G. Ecker and W. Weizel, Ann. Physik, Leipzig, 1956, 17, 126.

6. H.N. Olsen, Phys. Rev., 1961, 124, 1703.

7. H.R. Griem, Phys. Rev., 1962, 128, 997.

8. C.E. Moors, 'Atomic Energy Levels' Vol. 1, 2 and 3, Natl. Bur. Standards (U.S.), Circ. 467, 1949.

9. M. McChesney, Proc. Phys. Soc., 1964, 84, 983.

10. S. Chandrasekhar, 'Radiative Transfer', Dover Publications, New York, 1960.

11. R.G. Breene and M.C. Nardone, J. Quant. Spectr. Rad. Transfer, 1962, 2, 273.

12. A. Unsöld, "Physik Der Sternatmosphären", Springer-Verlag, Berlin, 1955, 2nd Edn.

13. H.A. Kramers, Phil. Mag., 1923, 46, 836.

14. H.E. Petschek, P.H. Rose, H.S. Glick, A. Kane and A. Kantrowitz, J. Appl. Phys., 1955, 26, 83.

15. H.E. Petschek and S. Byron, Ann. Phys. N.Y., 1957, 1, 270.

16. J.C. De Vos, Physica, 1954, 20, 690; G.A.W. Rutgers and J.C. De Vos, Physica, 1954, 20, 715.

/APPENDIX .....

APPENDIX

Symbols

T	temperature, °K
ρ	density, g cm^{-3}
u	velocity, cm sec^{-1}
M_A	atomic mass, g
M_e	electron mass, 9.1072×10^{-28} g
α	degree of ionization
χ	ionization potential, eV
R	gas constant per unit mass, ergs deg^{-1} g^{-1}
k	Boltzmann's constant, 1.3803×10^{-16} erg deg^{-1}
e	charge of electron, 4.803×10^{-10} esu
el	electronic
h	Planck's constant, 6.6237×10^{-27} erg sec
Q	partition function
P	pressure, dyn cm^{-2}
g_n	statistical weight
c	velocity of light, 2.9979×10^{10} cm sec^{-1}
N_e	electron density, cm^{-3}
I	intensity, erg cm^{-2}
K	absorption coefficient, cm^{-1}
σ	absorption cross-section, cm^{-2}
ϵ	emissivity

/Symbols (Cont'd.) .....

APPENDIX

Symbols (Cont'd.)

ν	frequency, sec^{-1}
ℓ	thickness of gas layer, cm
n	n^{th} term
N	density of absorbing gas particles, cm^{-3}
β	correction term for emissivity
$\bar{g}$	correction factor for absorption coefficient
B_ν	Planck black body function, erg cm^{-2}
τ_1	ionization relaxation time, 10^{-6} sec
1	gas behind shock wave
A	argon
Kr	krypton
Xe	xenon
He	helium
Ne	neon

Subscripts

o	undisturbed gas
1	gas behind shock wave

S. No. 985/67/CJ

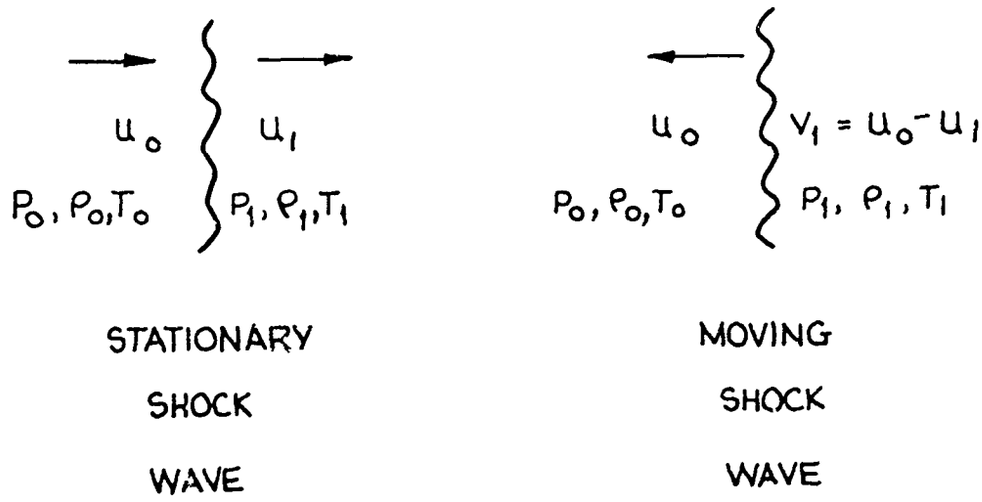

FIG. 1. FLOW REGIMES FOR STATIONARY AND MOVING SHOCK WAVES.

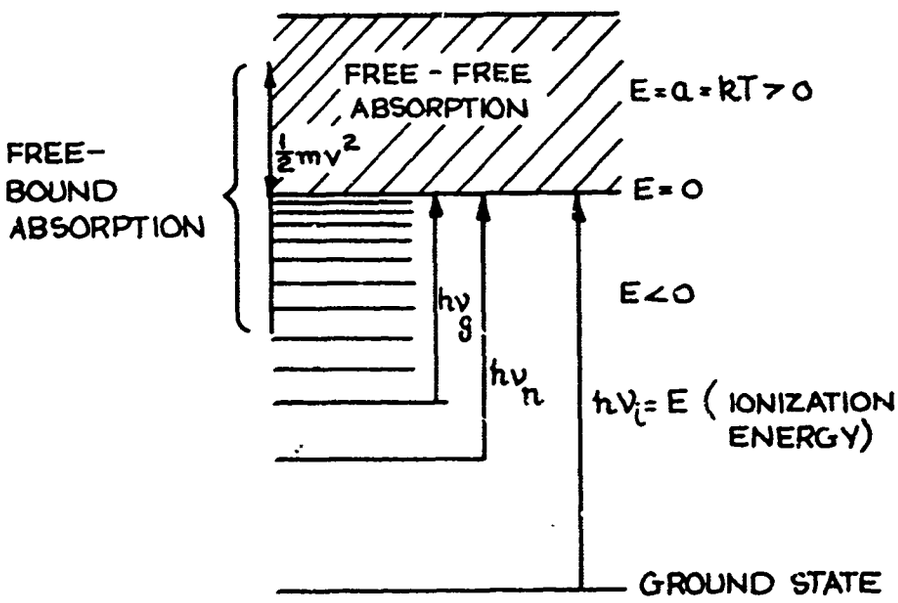

FIG. 2. MODEL TERM SCHEME FOR FREE-FREE AND FREE-BOUND ABSORPTION.

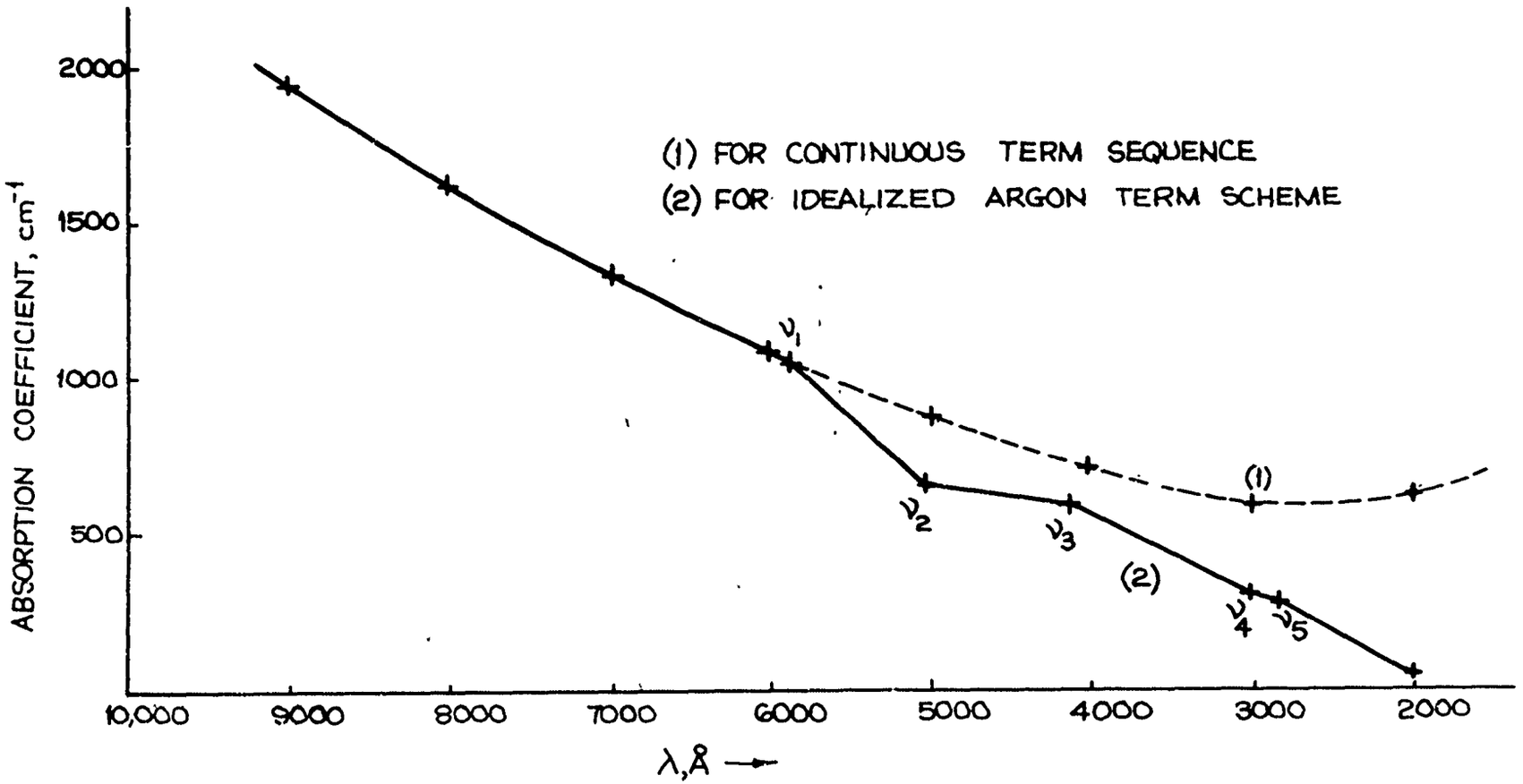

FIG.3. FREE-FREE AND FREE-BOUND ABSORPTION COEFFICIENT FOR ARGON.

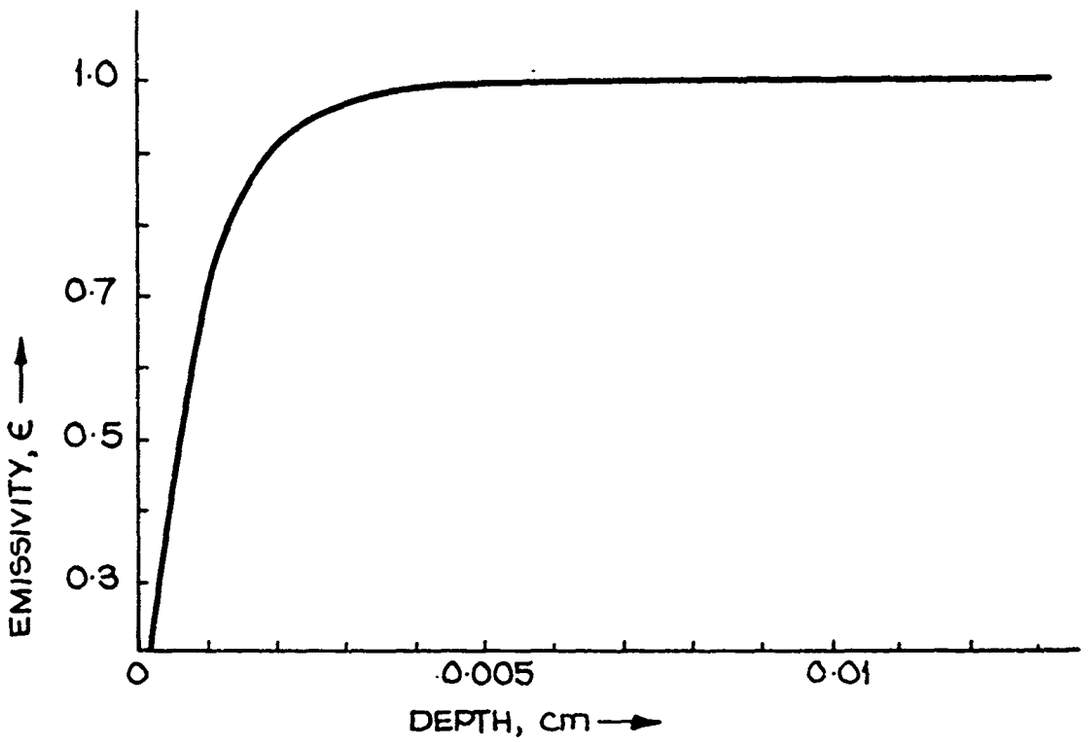

FIG. 4. EMISSIVITY AS A FUNCTION OF DEPTH FOR AN ARGON PLASMA AT 5000 Å.

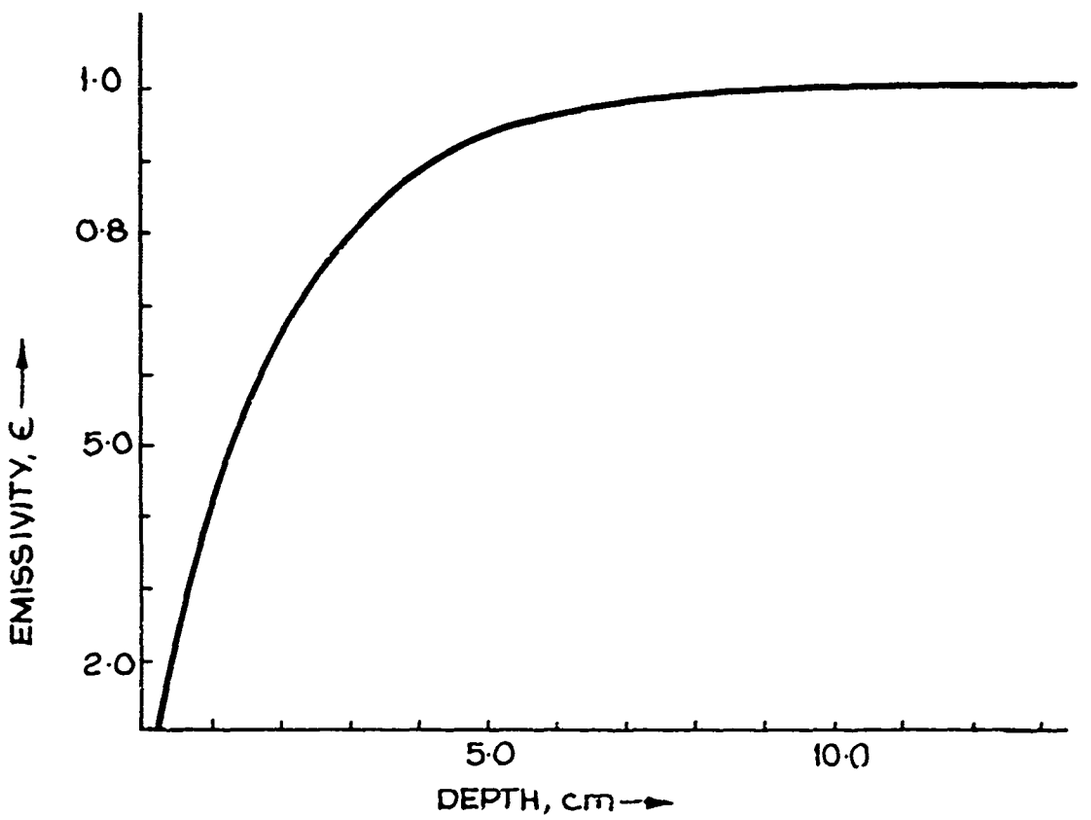

FIG. 5. EMISSIVITY CURVE FOR HELIUM BEHIND REFLECTED SHOCK.

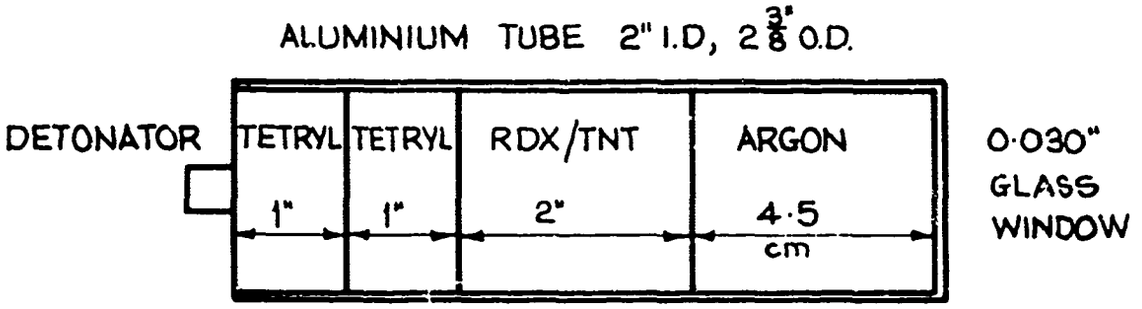

FIG. 6. SCHEMATIC DIAGRAM OF SHOT ASSEMBLY USING ATMOSPHERIC PRESSURE GASES.

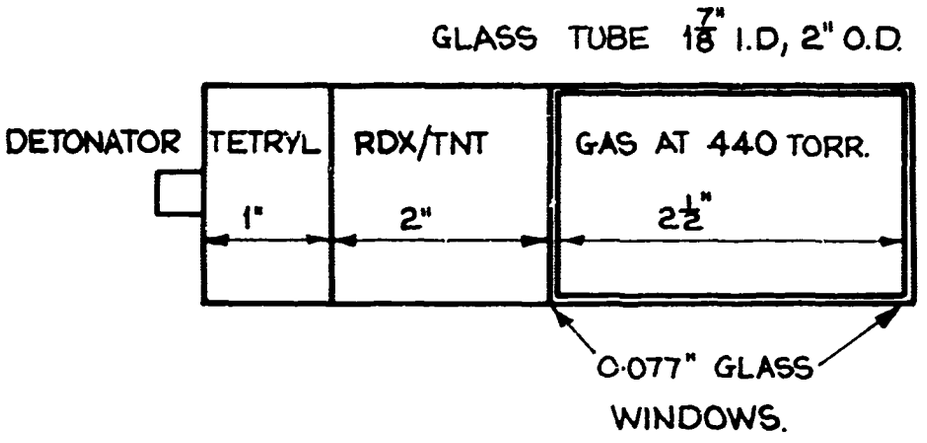

FIG. 7. SCHEMATIC DIAGRAM OF SHOT ASSEMBLY USING SPECTROSCOPIC GASSES AT 440 TORR.

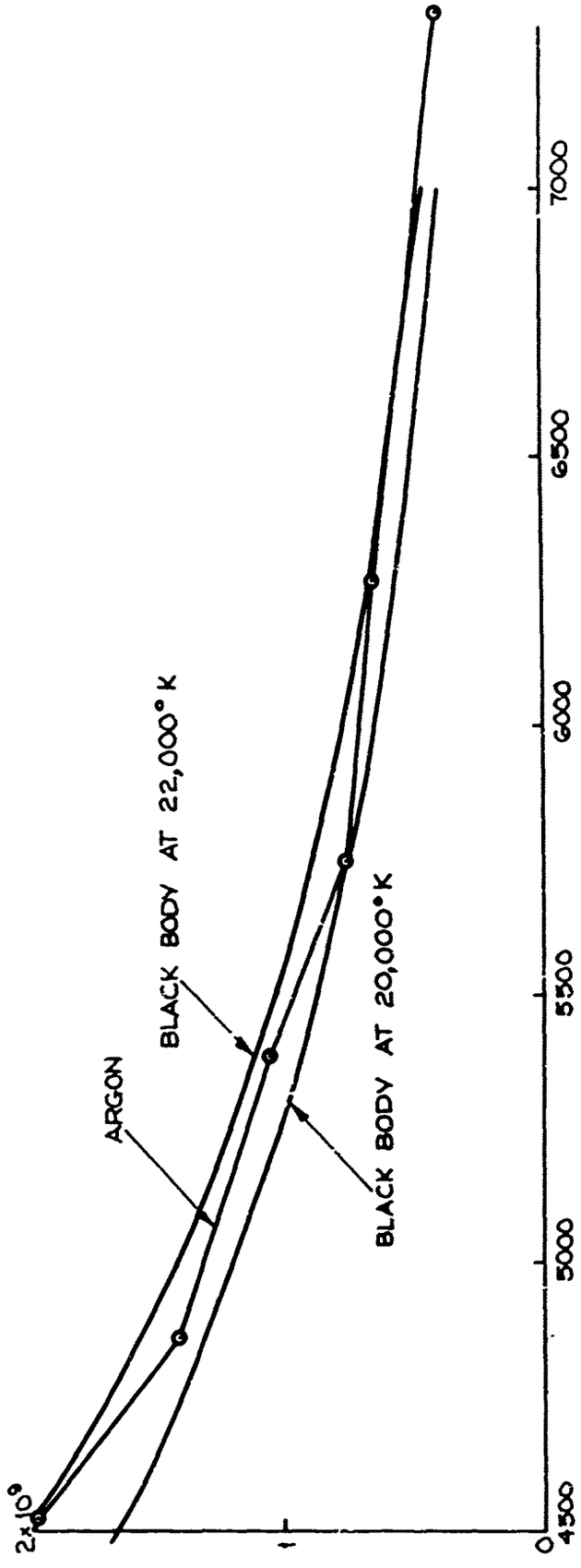

FIG. 8. SPECTRAL INTENSITY FOR ARGON SHOCKED BY RDX/TNT.

ERDE 12/R/67

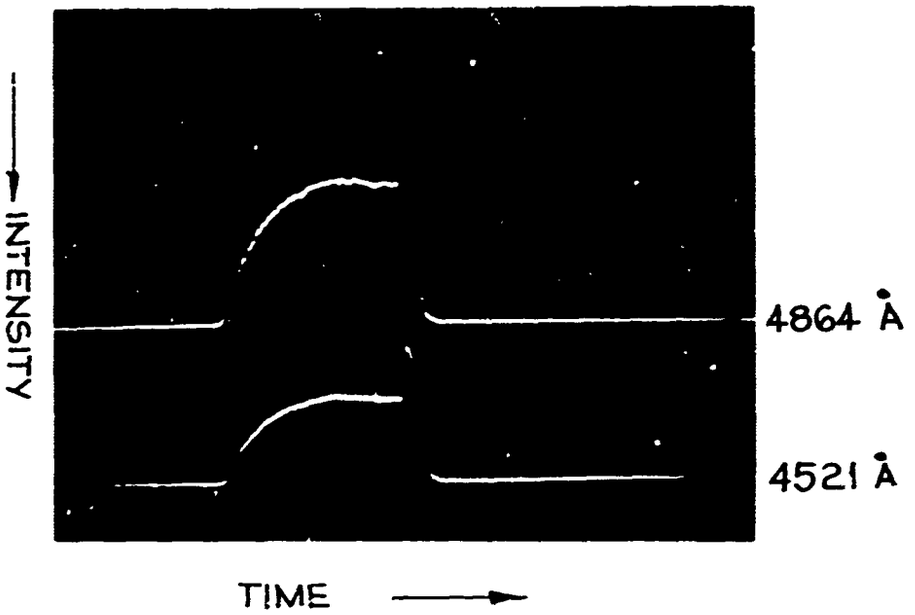

FIG. 9. PHOTOMULTIPLIER RECORD OF SPECTROSCOPIC ARGON SHOCK HEATED BY RT.

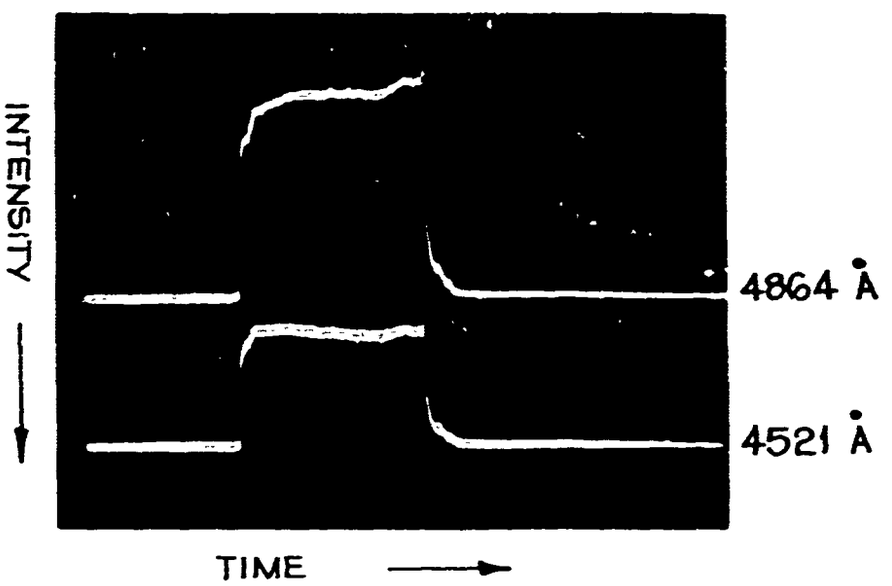

FIG. 10. PHOTOMULTIPLIER RECORD OF SPECTROSCOPIC XENON SHOCK HEATED BY RT.

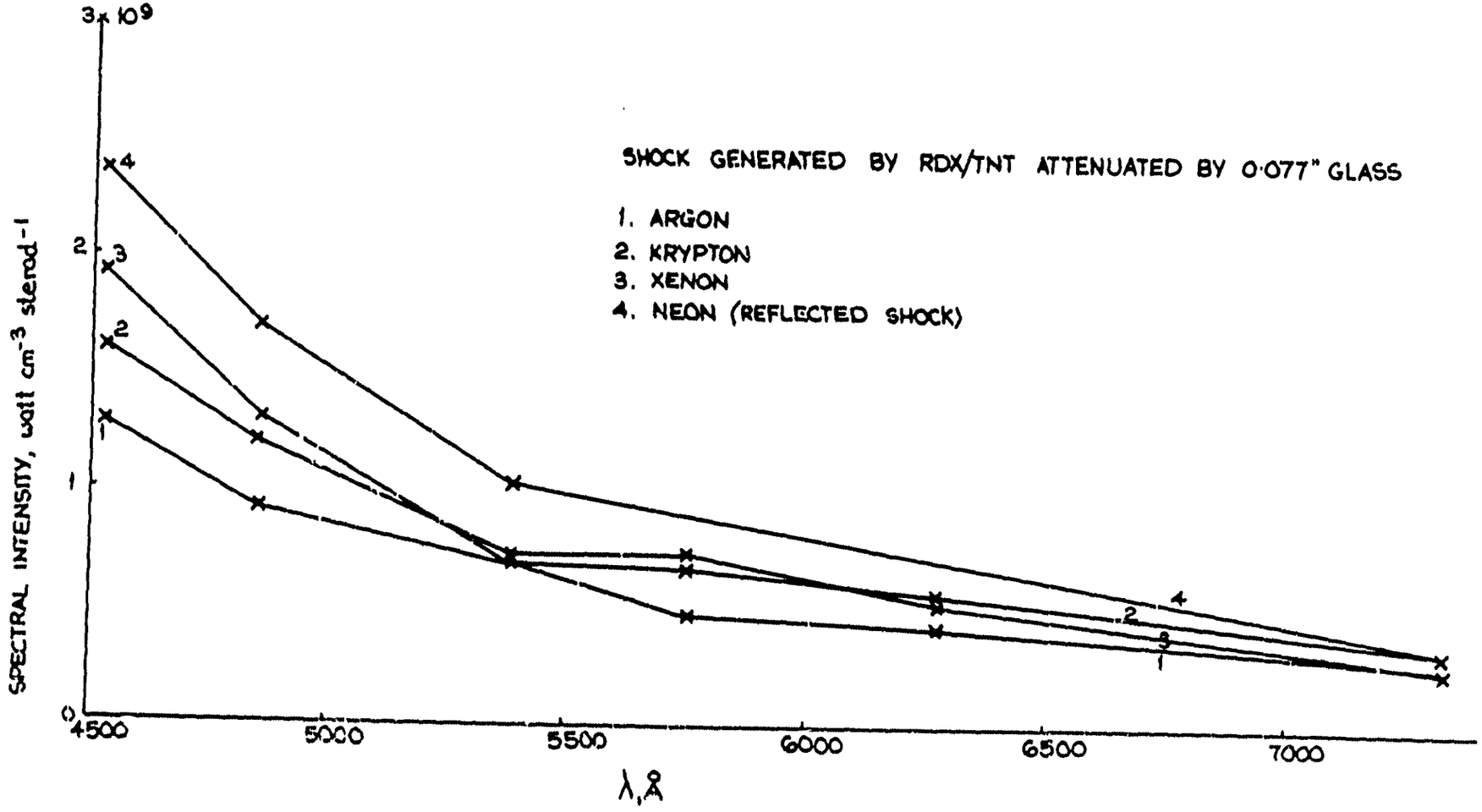

FIG. 11. SPECTRAL INTENSITY FOR RARE GASES SHOCKED BY RDX/TNT.

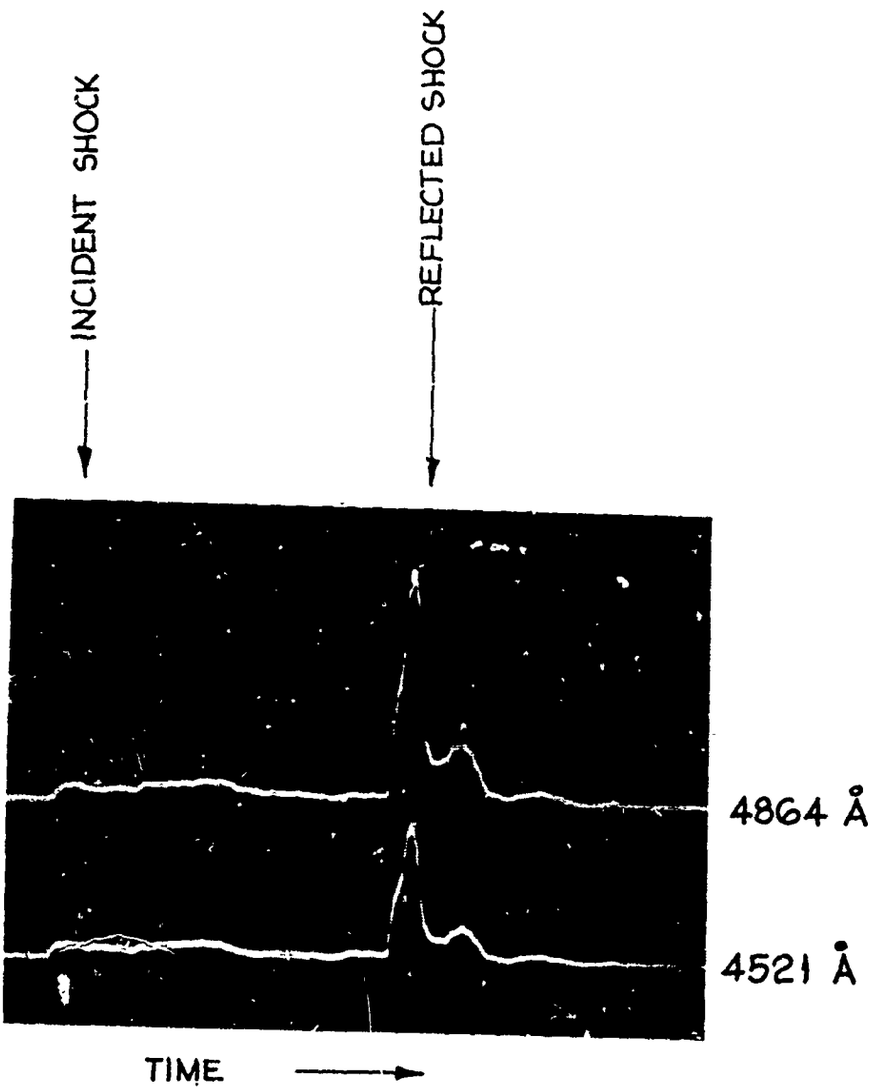

FIG. 12. PHOTOMULTIPLIER RECORD OF ATMOSPHERIC PRESSURE HELIUM SHOCK HEATED BY RT.

FIG. 13A. STREAK PHOTOGRAPH OF SHOCKED ARGON.

FIG. 13B. STREAK PHOTOGRAPH OF SHOCKED HELIUM.

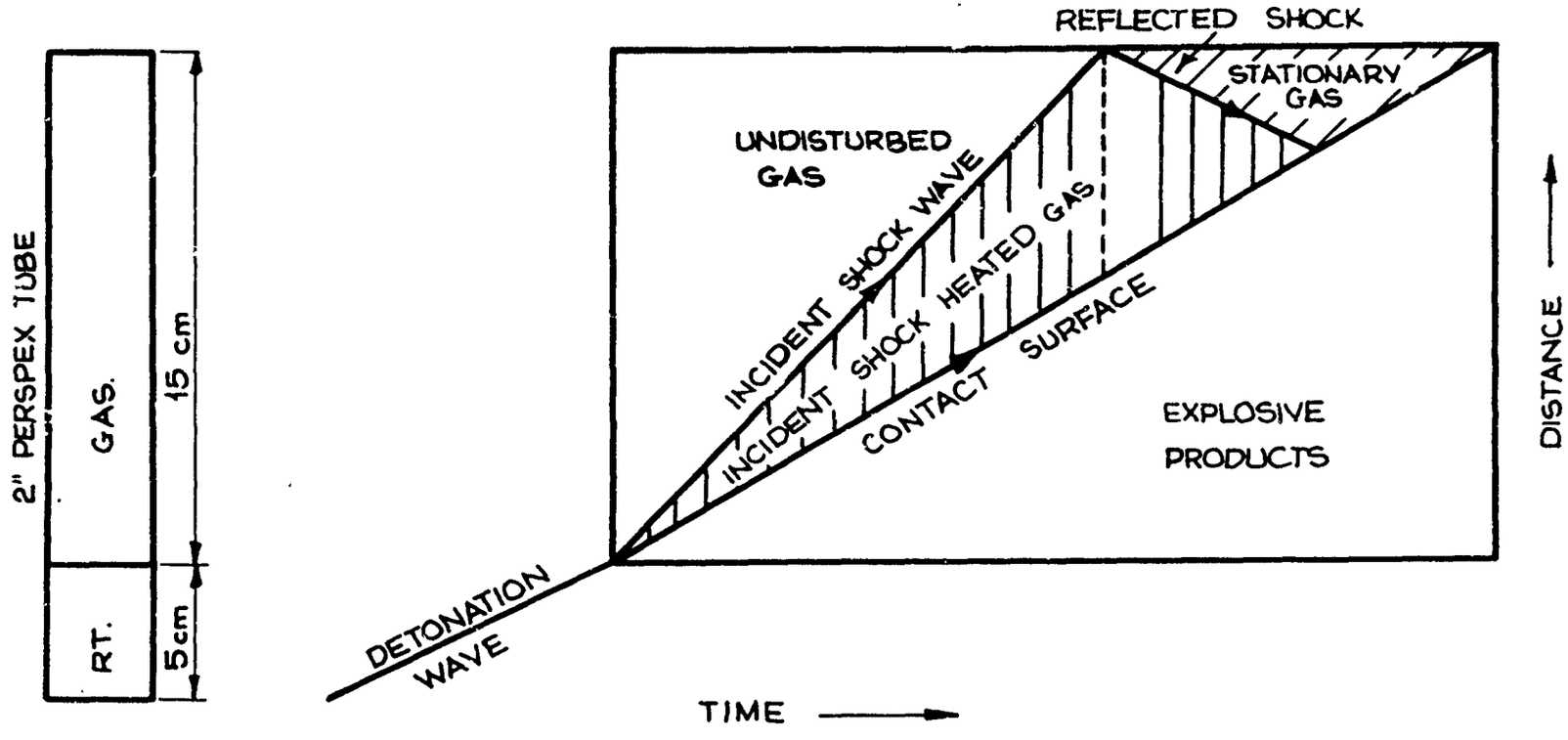

FIG. 14. TIME - DISTANCE DIAGRAM FOR INCIDENT AND REFLECTED SHOCK WAVE.

UNCLASSIFIED

ERDE Report No. 12/R/67 — High Explosive Light Sources as Possible Laser Pumps

R.T. Bailey and J.T.A. Burton November 1967

The visible radiation from a thermally ionized high density plasma produced by explosively generated shock waves has been investigated as a possible laser pumping source. It is considered that the major problem is the efficiency of conversion from chemical energy to radiation in the absorption band of the laser. The study has therefore been concentrated on the mechanism of the emissive process with a view to increasing the radiation emitted in a given spectral region. The real gas thermodynamic variables behind the shock waves have been evaluated for argon and helium and used to calculate linear absorption coefficients based on Unsöld-Kramers theory. Using Kirchhoff's law, the radiant intensities at the surfaces of optically thick argon and helium plasmas at 20,000°K have been calculated and compared /with .....

UNCLASSIFIED

UNCLASSIFIED

ERDE Report No. 12/R/67 — High Explosive Light Sources as Possible Laser Pumps

R.T. Bailey and J.T.A. Burton November 1967

The visible radiation from a thermally ionized high density plasma produced by explosively generated shock waves has been investigated as a possible laser pumping source. It is considered that the major problem is the efficiency of conversion from chemical energy to radiation in the absorption band of the laser. The study has therefore been concentrated on the mechanism of the emissive process with a view to increasing the radiation emitted in a given spectral region. The real gas thermodynamic variables behind the shock waves have been evaluated for argon and helium and used to calculate linear absorption coefficients based on Unsöld-Kramers theory. Using Kirchhoff's law, the radiant intensities at the surfaces of optically thick argon and helium plasmas at 20,000°K have been calculated and compared /with .....

UNCLASSIFIED

UNCLASSIFIED

ERDE Report No. 12/R/67 — High Explosive Light Sources as Possible Laser Pumps

R.T. Bailey and J.T.A. Burton November 1967

The visible radiation from a thermally ionized high density plasma produced by explosively generated shock waves ~~has been~~ investigated as a possible laser pumping source. It is considered that the major problem is the efficiency of conversion from chemical energy to radiation in the absorption band of the laser. The study has therefore been concentrated on the mechanism of the emissive process with a view to increasing the radiation emitted in a given spectral region. The real gas thermodynamic variables behind the shock waves have been evaluated for argon and helium and used to calculate linear absorption coefficients based on Unsöld-Kramers theory. Using Kirchhoff's law, the radiant intensities at the surfaces of optically thick argon and helium plasmas at 20,000°K have been calculated and compared /with .....

UNCLASSIFIED